JOURNAL OF AIRCRAFT
Vol. 32, No. 3, May–June 1995

Cooling of Aerospace Plane Using Liquid Hydrogen and Methane

Ahmed Z. Al-Garni,* Ahmet Z. Şahin,† Bekir S. Yılbaş,‡ and Saad A. Ahmed†
King Fahd University of Petroleum and Minerals, Dhahran 31261, Saudi Arabia

This work studies the active cooling for aerospace plane, using liquid hydrogen and liquid methane. The ascending optimized trajectory to minimize the heat load in the hypersonic part is used to perform the study. The study includes the cooling for the stagnation point, the leading edges for wings and engine and other parts of the aerospace plane that are close to the leading edges. Laminar flow for the stagnation point and both laminar and turbulent flow for the leading-edge heating have been considered. The amount of heat rate (total, radiative, and convective) and the mass of liquid coolant needed for cooling are calculated. A design of minimum inlet-outlet areas for the amount of liquid needed for cooling is made with the consideration of the coolant's physical constraints in liquid and gaseous states. The study shows that the ratio of masses of coolant to the initial total mass (initial total mass of the vehicle including fuel and coolant masses) are in the limit of the reachable range, which requires about 20% or less of initial total mass for cooling in the worst case. Comparison of liquid hydrogen and liquid methane shows that liquid hydrogen is a clearly superior candidate for coolant and it saves 10% of the initial total mass as compared to methane. The study shows that there are no fundamental barriers for the cooling system of the vehicle in terms of its coolant mass and area size for coolant passage.

Nomenclature

A	= area, m^2
a	= speed of sound, m/s
C_D	= drag coefficient
C_L	= lift coefficient
C_p	= specific heat at constant pressure at about 288.15 K and 1 atm, J/kg·K
C_Q	= heat constant, its units depend on the value of N' and M' in the heat rate equation
C_v	= specific heat at constant volume at about 288.15 K and 1 atm, J/kg·K
D	= drag, N
d	= width, m
g	= acceleration due to gravity, m/s^2
h	= geometric altitude, $(r - r_0)$, km
h_{ev}	= heat of vaporization at boiling point, J/kg
h_t	= total enthalpy, J/kg
h_w	= enthalpy at wall, J/kg
I_{sp}	= specific impulse, s
L	= lift, N
l	= length, m
M	= Mach number
M'	= number that represents the exponent of the velocity in the heat rate equation
m	= total mass of the vehicle including fuel and coolant masses at any time, kg
N'	= number that represents the exponent of the density in the heat rate equation
$\dot{Q}$	= heat rate per unit area, W/cm^2
R	= radius, m
R'	= gas constant at about 288.15 K and 1 atm, J/kg.K
Re	= Reynolds number
r	= vehicle position vector from earth center, m
T	= temperature, K
T_G	= coolant gas temperature at outlet of coolant path, a temperature higher than the boiling points temperature at 1 atm, K
T_L	= coolant liquid temperature at inlet of coolant path at about melting point and 1 atm, K
T_w	= wall temperature of the heating area without active cooling, K
T_{wr}	= wall temperature of about maximum radiation, 1500 K, K
t	= time, s
V	= velocity of the vehicle, m/s
X	= distance measured along the body surface from the body centerline, 4.0, m
X_T	= X for turbulent boundary layer, 4.0, m
β	= reciprocal of the scale height, ≈0.000147, 1/m
γ	= flight-path angle of the vehicle, rad
γ'	= ratio of specific heat at constant pressure-to-specific heat at constant volume, at about 288–293 K and 1 atm, C_p/C_v
ε	= surface emissivity for the material, 0.8
θ	= longitudinal position of the vehicle, rad
ν	= kinematic viscosity at about boiling point, m^2/s
ρ	= atmospheric air density as function of altitude, kg/m^3
ρ_G	= coolant gas density, a density higher than the boiling point density at 1 atm, kg/m^3
ρ_L	= coolant liquid density at about boiling point and 1 atm, kg/m^3
σ	= Stefan-Boltzmann constant, 5.67×10^{-8}, W/m^2 K^4
ϕ	= local body angle with respect to freestream, 45 deg

Subscripts

c	= convected
cl	= coolant
E	= engine
Ele	= engine leading edge
fl	= fuel

Received Sept. 22, 1993; revision received July 1, 1994; accepted for publication Sept. 15, 1994. Copyright © 1994 by the American Institute of Aeronautics and Astronautics, Inc. All rights reserved.

*Assistant Professor of Aerospace Engineering and Aeronautical Group Coordinator, Department of Mechanical Engineering. Member AIAA.

†Associate Professor, Department of Mechanical Engineering.

‡Professor, Department of Mechanical Engineering.

G	=	gas at outlet
h	=	heat
i	=	prefix for three cases, stagnation point, leading edges, and other parts
L	=	liquid at inlet
le	=	leading edge
max	=	maximum
max, rad	=	maximum radiation
min	=	minimum
min, il	=	minimum inlet
min, ol	=	minimum outlet
ot	=	other parts
radn	=	radiation
s	=	standard sea level
sp	=	stagnation point
T	=	turbulent
t	=	total, radiative plus convected
tl	=	total, stagnation point, leading edges, and other parts
W	=	wing
w	=	wall
wr	=	maximum wall radiation
0	=	initial at earth surface
∞	=	freestream

Introduction

IN this era, attention is being focused more and more upon hypersonic passenger aerospace planes in order to travel in space and reduce long distance flight times. However, during its flight through the atmosphere, such a vehicle will encounter high aerodynamic heating rates, which in turn produce high surface temperatures. Therefore, it will require an active cooling system for the stagnation point, leading edges, and some other parts of the wings-engine.

Tauber and Menees[1] have shown that the heat load of the stagnation point for the aerospace plane during ascent is about 10 times greater than the heating load of the Space Shuttle re-entry. The corresponding temperatures for such a high heating load vary from 3200 to 3800 K, which are far beyond the radiative cooling capabilities of existing, nonablating, heat shield materials. They have also indicated that the leading edge experienced high heating load with wall temperatures of 2250–2700 K. This shows that both the stagnation point and the wing leading edge may require some active cooling. However, the areas of the vehicle that require active cooling may be relatively small, and the radiative cooling should be effective over large areas of the aerospace plane.

Since severe heating occurs during ascent in the hypersonic flight, it poses major challenges for the cooling system design. Krause et al.[2,3] studied active thermal control for hypersonic vehicles. They presented a design and evaluation of a thermal control system that provided cooling by controlling the fuel flow through a network of heat exchangers. The study shows that efficient use of fuel cooling throughout the vehicles operating envelope requires modulating the flow paths within the network as the flight conditions change. Reich et al.[4] studied a thermal protection system (TPS) for hypersonic vehicles, which was required in order to limit the heat transfer into the central fuselage of liquid fuel. The study demonstrates that microporous and multiwall insulations are efficient, therefore, lightweight and reliable TPSs for future hypersonic vehicles can be designed. Rainey and Veziroglu[5] studied and compared the two cryogenic fuel candidates for a hypersonic vehicle: 1) liquid hydrogen and 2) liquid methane. The results show that the hydrogen-fueled hypersonic vehicle is superior to the methane-fueled one for long range of flight. In addition, the study shows that hydrogen is a safer fuel than methane.

In the present study, an active cooling computation is performed, which compares the amount of coolant mass needed with respect to the total mass and the amount of fuel mass needed through the envelope of the ascending trajectory in the hypersonic region. The study considers the amount of coolant, which is required for cooling the stagnation point region, leading edges of wing-engine, and other parts of larger area around the leading edges for an extreme case study. The study includes laminar flow over the stagnation point, laminar and turbulent flow over the leading edges, and other parts. The study also compares two candidates for cooling, namely liquid hydrogen and liquid methane. A model that consists of the ascending trajectory equations of motion is used in this study, which is similar to the one used by Vinh.[6] The trajectory used for this study is the same as the one presented by Al-Garni and Barlow (Refs. 7 and 8), which minimizes the heat load on the aerospace plane. Apparently, no unclassified studies have been performed in this specific area with the above stated conditions of flight. Therefore, contributions in this area are very much needed.

Model Equations

The vehicle is modeled as a point variable mass with parabolic drag polar and variable lift and thrust as described in the previous study.[7] The earth is assumed spherical, nonrotating with an exponential atmosphere. The trajectory is taken in the equatorial plane. With the above assumptions, the equations that describe the ascending hypersonic trajectory have the following form:

$$\frac{\mathrm{d}r}{\mathrm{d}t} = V \sin \gamma \tag{1}$$

$$\frac{\mathrm{d}\rho}{\mathrm{d}t} = -\rho \beta V \sin \gamma \tag{2}$$

$$\frac{\mathrm{d}V}{\mathrm{d}t} = \frac{(T_t - D_t)}{m} - g \sin \gamma \tag{3}$$

$$V \frac{\mathrm{d}\gamma}{\mathrm{d}t} = \frac{L_t}{m} - g \cos \gamma + \frac{V^2}{r} \cos \gamma \tag{4}$$

$$\frac{\mathrm{d}m}{\mathrm{d}t} = -\frac{T_t}{(I_{sp} g_0)} \tag{5}$$

$$\frac{\mathrm{d}Q_t}{\mathrm{d}t} = C_Q \rho^{N'} V^{M'} \tag{6}$$

where the heat coefficient C_Q, N', and M' found in Refs. 1 and 9 are as follows:

For a stagnation point; $N' = 0.5$, $M' = 3$

$$C_Q = 1.83 \times 10^{-8} R_{sp}^{-0.5}[1 - (h_w/h_0)] \tag{6a}$$

For leading edges and other parts;

if treated as laminar flat plate; $N' = 0.5$, $M' = 3.2$

$$C_Q = 2.53 \times 10^{-9} (\cos \phi)^{0.5} (\sin \phi) X^{0.5} [1 - (h_w/h_0)] \tag{6b}$$

if treated as turbulent flat plate

for $V_\infty \leq 3962$, $N' = 0.8$, $M' = 3.37$

$$C_Q = 3.89 \times 10^{-8} (\cos \phi)^{1.78} (\sin \phi)^{1.6} X^{-0.2} \times (T_{wr}/556)[1 - 1.11(h_w/h_t)] \tag{6c}$$

for $V_\infty > 3962$, $N' = 0.8$, $M' = 3.7$

$$C_Q = 2.2 \times 10^{-9} (\cos \phi)^{2.08} (\sin \phi)^{1.6} X_T^{-0.2} \times [1 - 1.11(h_w/h_t)] \tag{6d}$$

Table 1 Input data[10-13]

Coolant	h_{ev}	C_p	T_0	ν	ρ_L	ρ_G	γ'	R'
H_2	451,900	14,200	14.01	1.5714×10^{-7}	70	1.329	1.41	4127
CH_4	577,400	2,253.7	90.67	3.686×10^{-7}	424	1.8004	1.31	518.35

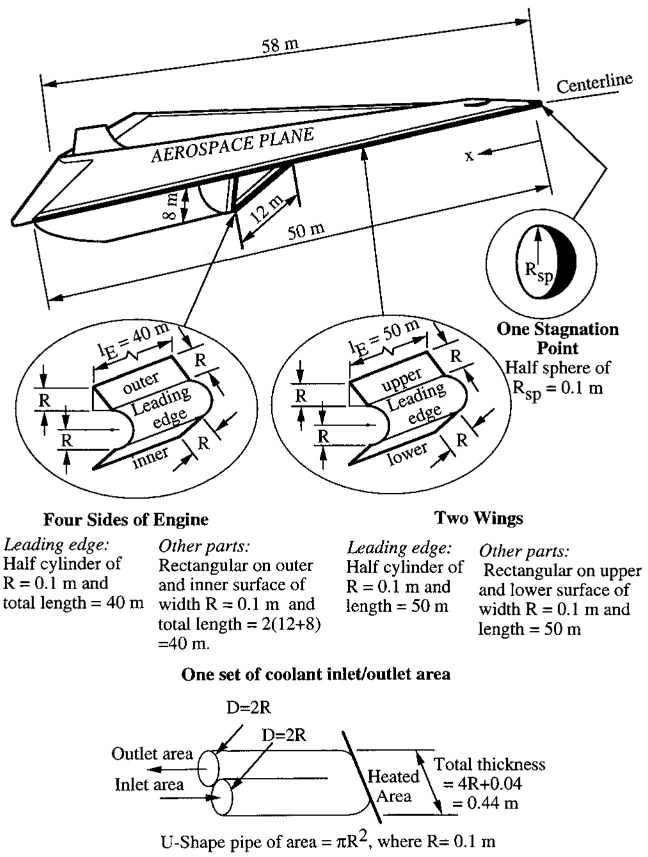

Fig. 1 Aerospace plane and its cooling system.

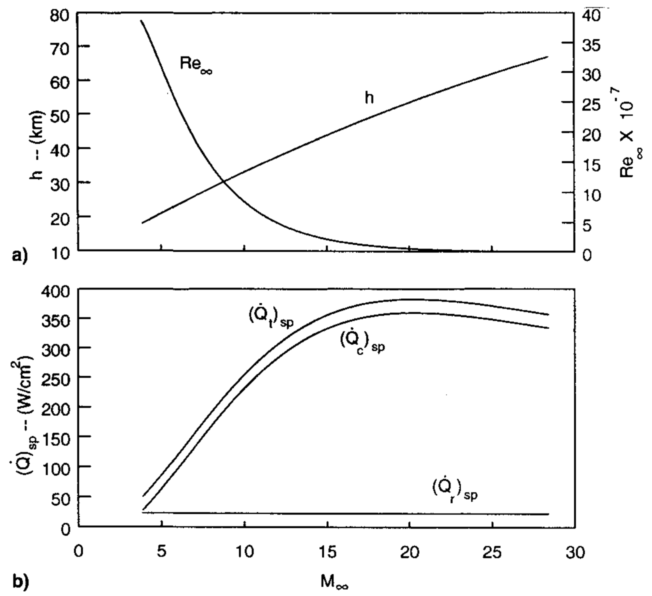

Fig. 2 a) h and Re_∞ vs M_∞ and b) $(\dot{Q})_{sp}$ vs M_∞.

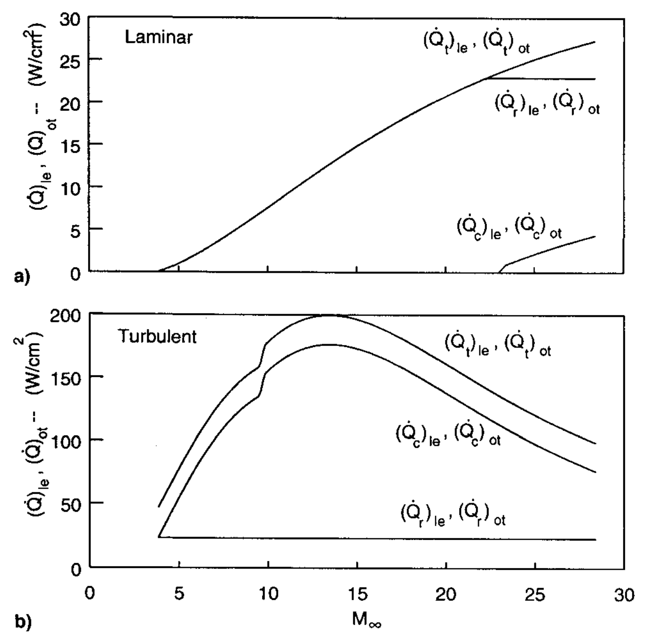

Fig. 3 $(\dot{Q})_{le}$ and $(\dot{Q})_{ot}$ for a) laminar case vs M_∞ and b) for turbulent case vs M_∞.

taking ϕ = 45 deg (this gives the extreme value of heat generation), $X = X_T = 4.0$ m from the centerline $(h_w/h_0) = 0.1$, and T_{wr} = 1500 K. Note that we add the above six equations [Eqs. (1–6)] to the mass rate of coolant, Eq. (12) to complete the system of equations to be integrated.

The wall temperature

$$T_w = (\dot{Q}_t/\varepsilon\sigma)^{0.25} \tag{7}$$

where $\varepsilon = 0.8$ and $\sigma = 5.67 \times 10^{-8}$.

Considering that

if $T_w \leq 1500$ K, then all the heat will be radiated, i.e., $\dot{Q}_{rad} = \dot{Q}_t$

if $T_w > 1500$ K, then

$$(\dot{Q}_c)_i = (\dot{Q}_t)_i - \dot{Q}_{max,rad} \tag{8}$$

where $\dot{Q}_{max,rad} = 23$ is the maximum radiation at $T_w = 1500$ K and i represents three cases: 1) the stagnation point, 2) the leading edges, and 3) other parts. Note that $\dot{Q}_c$ is the same for leading edges and other parts.

In the heated area $(A_h)_i$, in Fig. 1, where i represents the three cases defined as follows:

1) For the stagnation point, the heated area is taken as half the area of the sphere with radius R_{sp}. This gives

$$(A_h)_{sp} = 2\pi R_{sp}^2 \tag{9}$$

where $R_{sp}(= 0.1\text{ m})$ is the radius of the sphere.

2) For the leading edge, the heated area is taken as the surface area of a half cylinder with radius R_{sp} along the leading edge of the two wings $(2l_{W\text{le}})$ and four engine sides $(l_{E\text{le}})$. This gives

$$(A_h)_{\text{le}} = \pi R_{sp}(2l_{W\text{le}} + l_{E\text{le}}) \tag{10}$$

where $l_{W\text{le}}$ = 50 m for each wing and $l_{E\text{le}}$ = 40 m for four sides of the edges of the engine.

3) The heated area for other parts is considered to consist of rectangular areas that are next to the leading edges of the two wings and four sides of the engines. The two sides of the

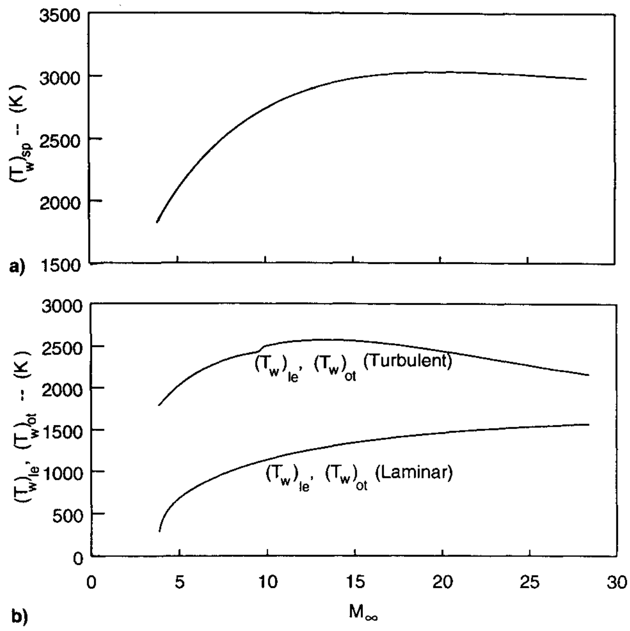

Fig. 4 a) $(T_w)_{sp}$ vs M_∞ and b) $(T_w)_{le}$, $(T_w)_{ot}$ vs M_∞.

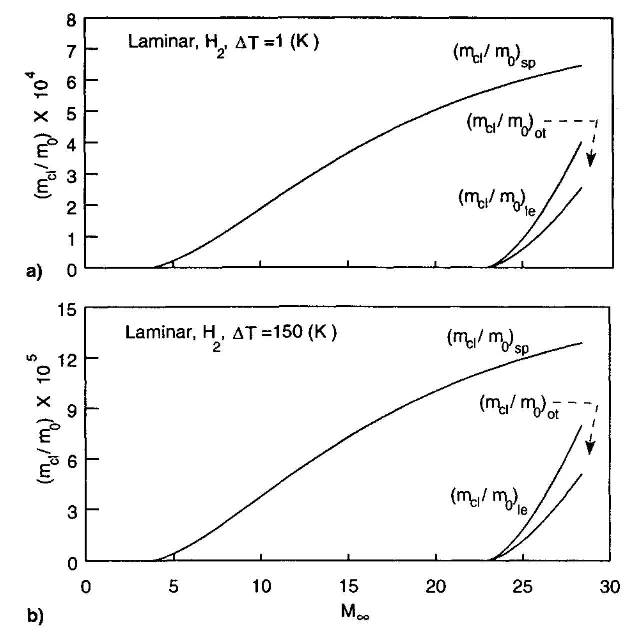

Fig. 5 (m_{cl}/m_0) for H_2, ΔT = a) 1 and b) 150 vs M_∞.

rectangular area have widths $d = R_{sp} = 0.1$ m and the total length of leading edges is $(2l_{W\text{le}} + l_{E\text{le}})$. This gives

$$(A_h)_{\text{ot}} = 2d(2l_{W\text{le}} = l_{E\text{le}}) \tag{11}$$

The coolant mass rate to cool the heated area is given by

$$(\dot{m}_{\text{cl}})_i = \frac{(\dot{Q}_c)_i(A_h)_i}{h_{e_v} + C_p(\nabla T)_i} \tag{12}$$

where $(\Delta T) = (T_G) - (T_L)$; noting that the units of $\dot{Q}_c$ by A_h should be in watts, in Eq. (12), with i representing three cases: 1) stagnation point, 2) leading edges, and 3) other parts. Equation (12) will be added to the first six equations of the system, which will be integrated numerically.

To design the inlet/outlet areas for the coolant one should, at least, get the minimum area for both from the following:

$$(A_{\text{min,il}})_i = (1/\pi)[2(\dot{m}_{\text{cl}})_i/\rho_L \nu Re_{\text{max}}]^2 \tag{13}$$

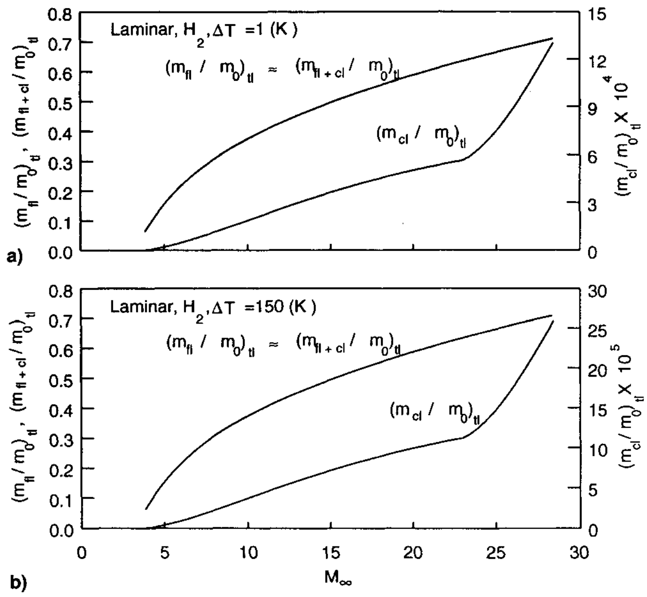

Fig. 6 $(m_{fl}/m_0)_{tl}$, $(m_{fl+cl}/m_0)_{tl}$ for H_2, ΔT = a) 1 and b) 150 vs M_∞.

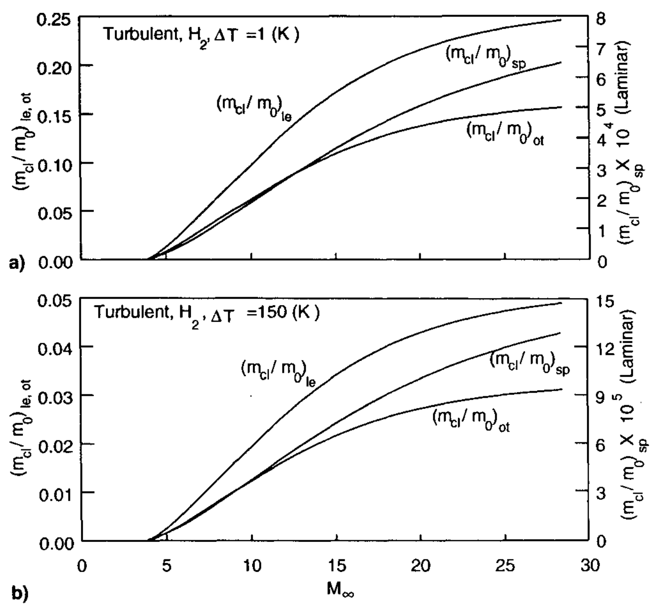

Fig. 7 $(m_{cl}/m_0)_{le,ot}$ for H_2, ΔT = a) 1 and b) 150 vs M_∞.

where for the design of the inlet area we have used the maximum possible Reynolds number in a pipe ($Re_{\text{max}} = 3.2 \times 10^6$, see Ref. 10) in liquid state. For the design of the outlet area, the flow Mach number is taken as 65% of the speed of sound for any outlet shape considering the coolant to be in a gaseous state. This provides flow Mach numbers less than the critical Mach number and avoids the shocks occurring in the flow. Thus

$$(A_{\text{min,ol}})_i = (\dot{m}_{\text{cl}})_i/\rho_G 0.65(a_G) \tag{14}$$

where $a_G = \sqrt{\gamma' R' T_G}$. Noting that Mach number $M = V/a_s$, where $a_s = 340$ m/s at standard sea level.

Figure 1 shows the aerospace plane, the three types of heated areas, and one set of the inlet/outlet areas for the coolant. Noting that the inlet/outlet areas for coolant can be divided into small set of areas, where each set of these consists of U-shaped pipes with cross-sectional area $= \pi(D/2)^2$ with $D = 0.2$ m. Furthermore, the set of areas along the wing and the engine sides have a total length of 140 m, which can be divided by $2D + 0.4$ (pipe thickness). This in turn gives a total of about 318 sets of areas for leading edge and the same for other parts. Consequently, a maximum allowable coolant area of 9.985 m^2 (0.0314 m^2 $\times$ 318 = 9.985 m^2) results for inlet/outlet areas of leading edges and the same for the other parts.

Input data: the aerospace plane data is taken from the early studies[7,8] such that, the initial total mass m_0 = 454,000 kg, total length of the vehicle = 58 m, aerodynamic reference area of the vehicle = 860 m^2, length for each wings leading edge (considering the worst case) $l_{W\mathrm{le}}$ (=50 m), and total length for four sides of engine leading edges, $l_{E\mathrm{le}}$ (=40 m) (considering the worst case). The physical properties of the coolant are taken from Refs. 11–14 and are shown in Table 1. The study considered the general trends with ΔT as a parameter (e.g., 1 and 150 K), where $T_G = T_L + \Delta T$.

Results and Discussions

Results obtained from the study are for the two coolants: 1) liquid hydrogen and 2) liquid methane, for laminar and turbulent flow and for the temperature gradient of ΔT = 1 and 150 K. The results are shown in Figs. 2–18 for the trajectory h, Reynolds number Re_∞, total heat rate $\dot{Q}_t$, convected heat rate $\dot{Q}_c$, radiative heat rate $\dot{Q}_r$, wall temperature T_w, mass ratio of coolant and fuel plus coolant with respect to initial total mass m_{cl}/m_0 and $m_{\mathrm{fl+cl}}/m_0$, and minimum areas required for inlet A_{il} and outlet A_{ol} of coolant mass flow for different flow conditions and temperature change ΔT. This is carried out for the stagnation point, leading edges, and other parts.

The general results show that turbulent flow generates more heat rate and load than laminar flow, hence, it requires more coolant mass and larger inlet/outlet area for coolant passage than that for laminar flow. The increase in the parameter ΔT reduces the required mass of coolant and the coolant inlet/outlet areas. The comparison of hydrogen and methane shows hydrogen gives better results than methane as a coolant.

The change in temperature ΔT is taken to be a parameter. Two situations have been studied: 1) ΔT (=1 K) and 2) ΔT (=150 K). The first situation with ΔT (=1 K) is not practical, because the temperature of the coolant will have sufficient time to reach much higher temperatures when it contacts the

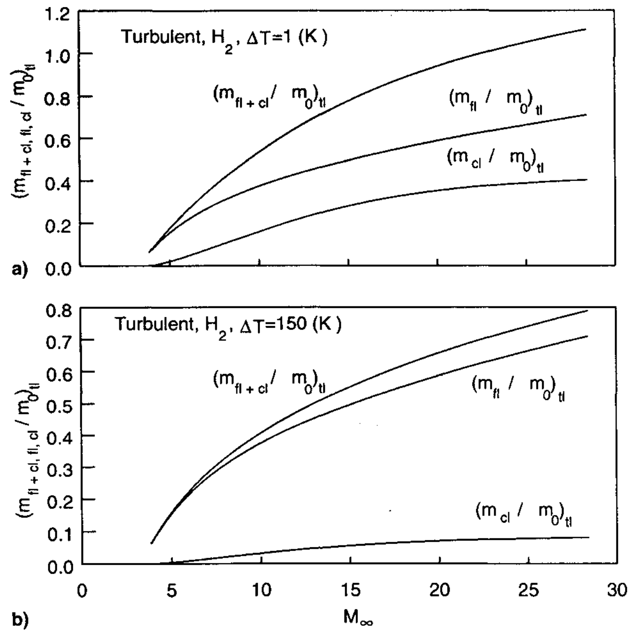

Fig. 8 $(m_{\mathrm{fl+cl,fl,cl}}/m_0)_{\mathrm{tl}}$ for H_2, ΔT = a) 1 and b) 150 vs M_∞.

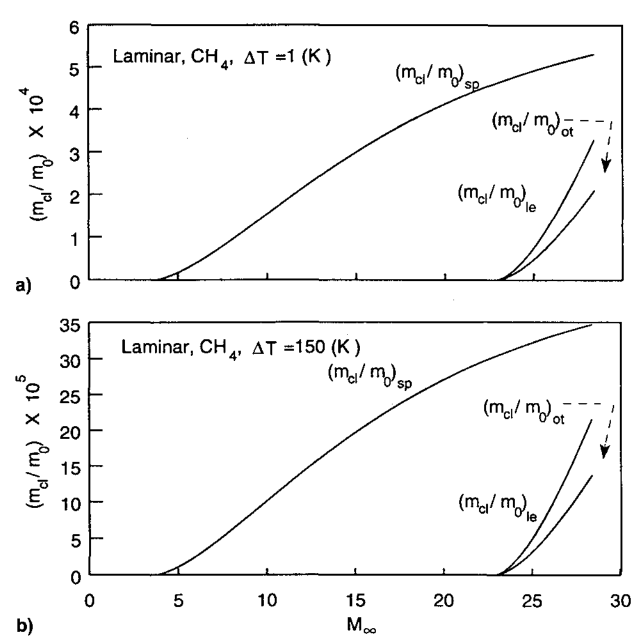

Fig. 9 (m_{cl}/m_0) for CH_4, ΔT = a) 1 and b) 150 vs M_∞.

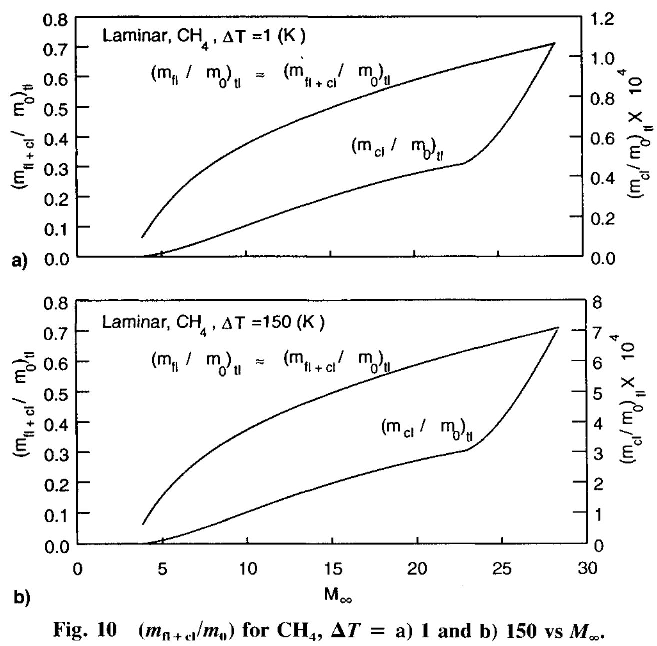

Fig. 10 $(m_{\mathrm{fl+cl}}/m_0)$ for CH_4, ΔT = a) 1 and b) 150 vs M_∞.

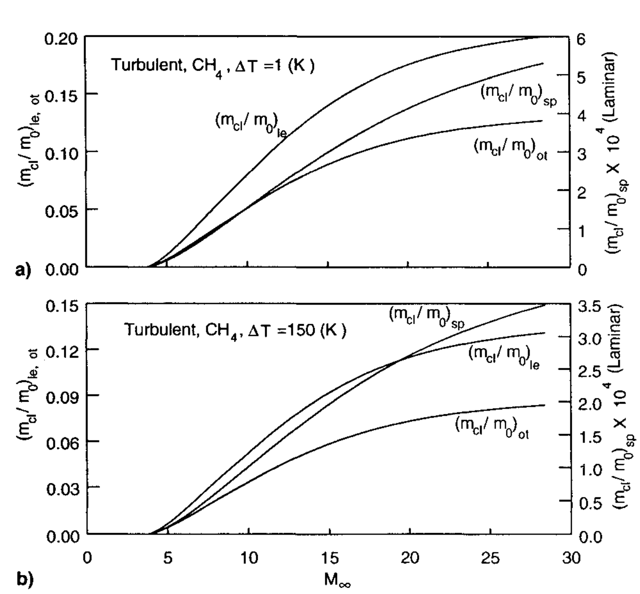

Fig. 11 $(m_{\mathrm{cl}}/m_0)_{\mathrm{le,ot}}$ for CH_4, ΔT = a) 1 and b) 150 vs M_∞.

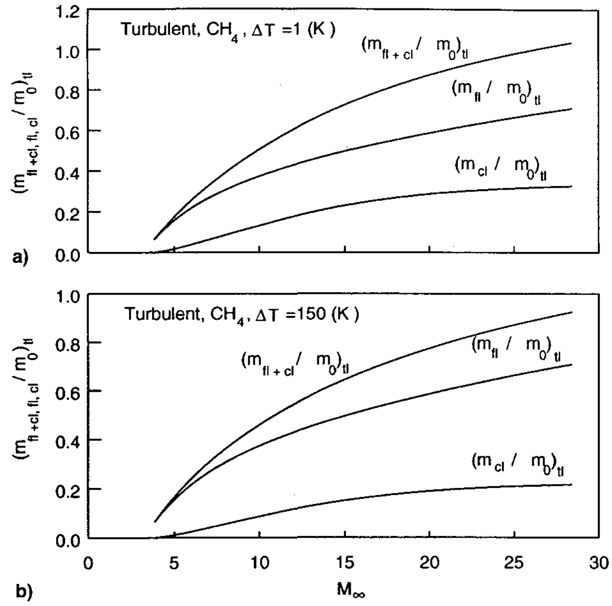

Fig. 12 $(m_{fl+cl,fl,cl}/m_0)_{tl}$ **for** CH_4, ΔT **= a) 1 and b) 150 vs** M_∞**.**

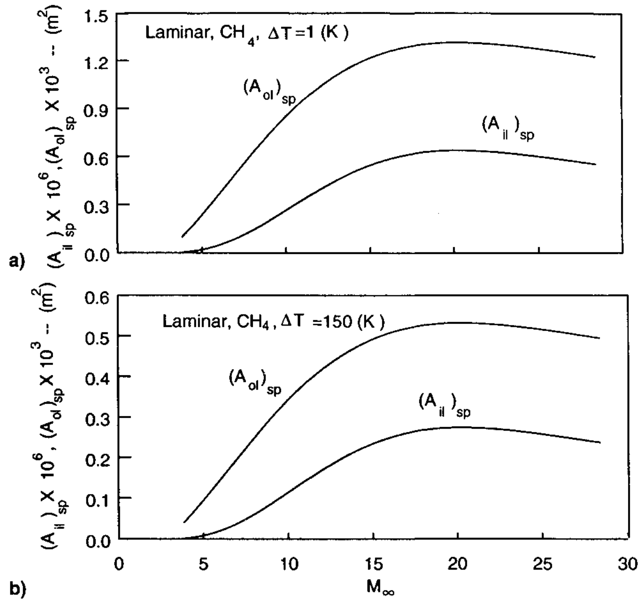

Fig. 14 $(A_{il})_{sp}$, $(A_{ol})_{sp}$ **for** CH_4, ΔT **= a) 1 and b) 150 vs** M_∞**.**

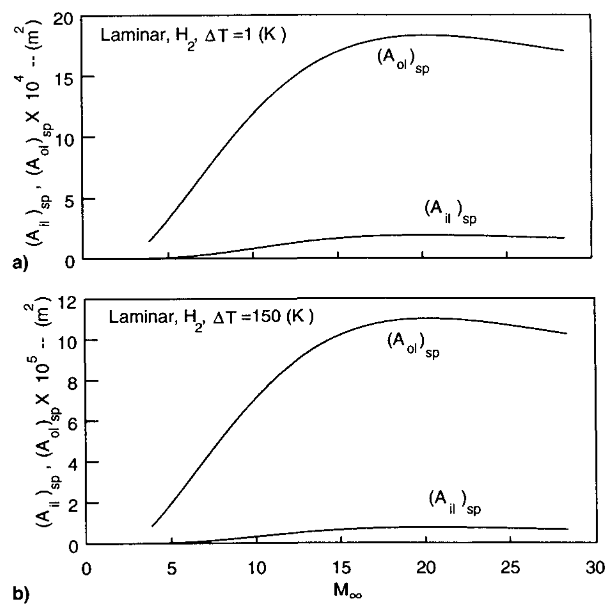

Fig. 13 $(A_{il})_{sp}$, $(A_{ol})_{sp}$ **for** H_2, ΔT **= a) 1 and b) 150 vs** M_∞**.**

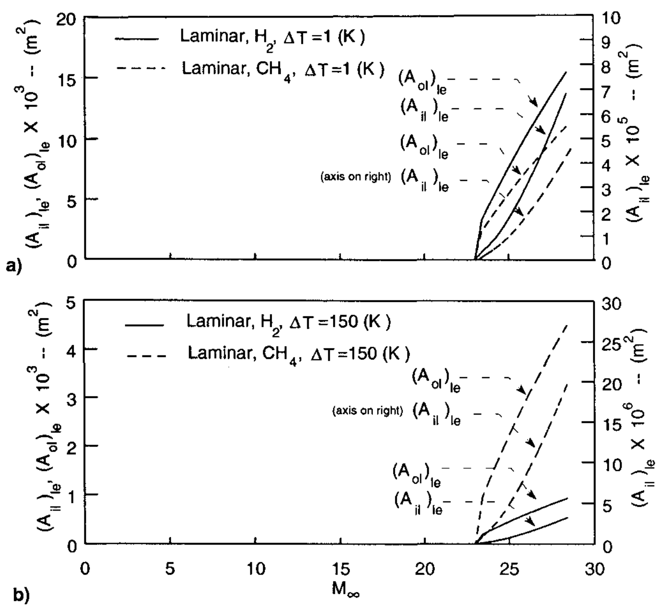

Fig. 15 $(A_{il})_{le}$, $(A_{ol})_{le}$ **for** H_2 **and** CH_4, ΔT **= a) 1 and b) 150 laminar cases vs** M_∞**.**

heated area, which has a very high temperature. The reason for introducing the first case is to show the effect of the change in temperature, which is an important parameter affecting the results. The second situation with ΔT (= 150 K) is more realistic, where the temperature of the coolant will come closer to room temperature (i.e., close to 300 K). The results of this case are more practically viable and, hence, taken seriously. The results of higher temperature changes (e.g., ΔT = 200 K) can be deduced by looking to the two cases of ΔT (= 1 and 150 K), which give a general trend.

The important results are obtained for mass ratios (both coolant and fuel) with respect to initial total mass for the stagnation point, leading edges, and other parts as shown in Figs. 5–12. The worst case of turbulent flow using high ΔT (= 150 K) needs a total coolant mass for liquid methane more than 20% of the initial total mass m_0. If we add to this the fuel mass (which has been calculated in Refs. 7 and 8, we need more than 90% of the initial total mass, which will leave less than 10% of initial total mass as payload and vehicle mass without fuel and coolant (see Fig. 12). In a similar situation if liquid hydrogen is used, less than 10% of the initial total mass is needed as coolant, which will consequently leave more than 20% of initial total mass as mass of aerospace plane and its payload without fuel and coolant (see Fig. 8). This shows that liquid hydrogen is clealy a better coolant compared to liquid methane since there is a difference in final mass of more than 10% of the initial total mass m_0.

The areas required for coolant are shown in Figs. 13–18. The following general trends are observed:

1) The area related to coolant inlet/outlet is directly proportional to the mass rate of coolant, which in turn is inversely proportional to the change in temperature ΔT.

2) The inlet area is smaller than the outlet area. For the same mass rate of the coolant at inlet/outlet, the areas will be inversely proportional to density, noting that the density of the liquid at the inlet is larger than the density of the gas at the outlet. This observation is true for all cases except for hydrogen, turbulent flow, because the ratio of $(\dot{m}_{cl}/\rho_L)^2 > (\dot{m}_{cl}/\rho_G)$.

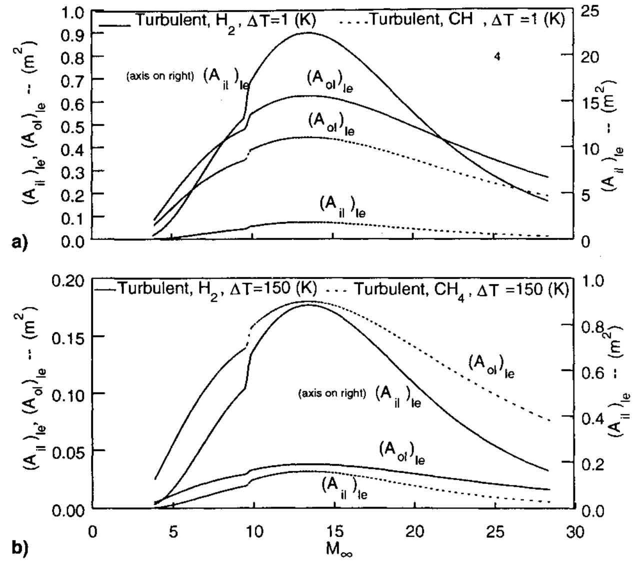

Fig. 16 $(A_{il})_{le}$, $(A_{ol})_{le}$ for H_2 and CH_4, ΔT = a) 1 and b) 150 turbulent cases vs M_∞.

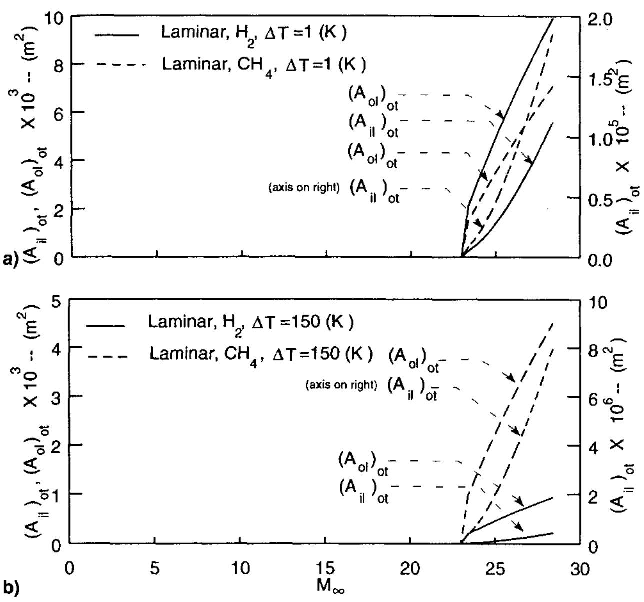

Fig. 17 $(A_{il})_{ot}$, $(A_{ol})_{ot}$ for H_2 and CH_4, ΔT = a) 1 and b) 150 laminar cases vs M_∞.

3) For a small change in temperature ΔT (=1 K) the areas at inlet and outlet are larger for liquid hydrogen than that for liquid methane. This is due to the fact that hydrogen has a lower density than methane at the inlet and outlet and because the area is inversely proportional to the density. This shows some advantage of liquid methane over liquid hydrogen, but this is not strictly true when we consider a large temperature gradient ΔT (more realistic), which will be discussed next.

4) For a large gradient of temperature ΔT (=150 K) the inlet areas for hydrogen are larger than that for liquid methane. This is due to the fact that the liquid hydrogen density is lower than that for liquid methane, in spite of the fact that the mass flow of hydrogen is less than methane. This is due to the fact that the difference in mass flow is less than the difference in liquid density between the two coolants. This advantage of methane over hydrogen becomes less important, since for turbulent flow (the worst case), we have the leading edges inlet area of 0.9 m^2 for liquid hydrogen, which is small enough and will not cause any serious problem, whereas for methane we need a corresponding area of 0.01 m^2, which is very small indeed (see Fig. 16). At the outlet we have a smaller area for hydrogen than methane. This is due to the fact that the mass flow rate required for methane is larger than that required for hydrogen, and also because the difference in mass flow is more than the difference in densities at gaseous state of the coolants, this shows an advantage of hydrogen over methane.

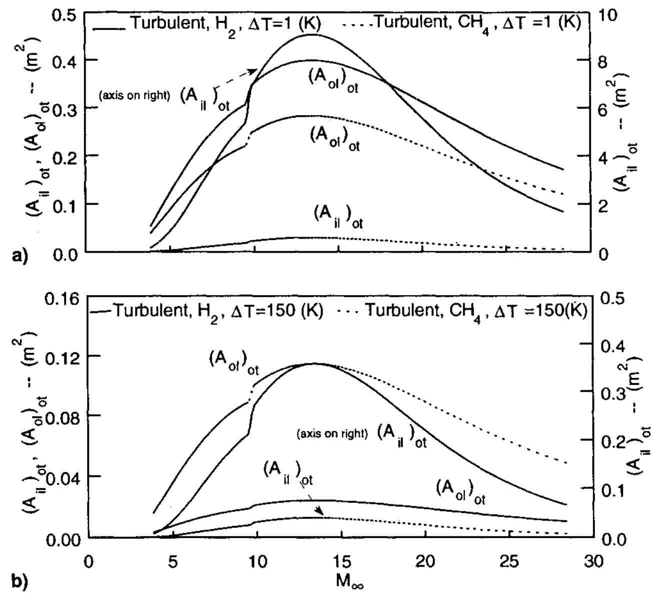

Fig. 18 $(A_{il})_{ot}$, $(A_{ol})_{ot}$ for H_2 and CH_4, ΔT = a) 1 and b) 150 turbulent cases vs M_∞.

The general results show that there is no fundamental problem in cooling the aerospace plane in terms of mass of coolant required and also in terms of the areas needed for coolant mass flow passage. Liquid hydrogen proves to be a clearly superior choice over liquid methane as a coolant, especially if considering the mass required for cooling. Liquid hydrogen will save more than 10% of the initial total mass m_0 compared to methane.

Conclusions

The study compares two coolants for an aerospace plane: 1) liquid hydrogen and 2) liquid methane. It is found from this study that their is no fundamental problem occurring in cooling the aerospace plane in terms of the coolant mass required and the areas needed for coolant mass flow passage.

The liquid hydrogen proves to be a better coolant than liquid methane. The amount of coolant using liquid hydrogen is less by 10% of initial mass total (for the worst case) than that using liquid methane.

Acknowledgment

The authors acknowledge the support of King Fahd University of Petroleum and Minerals, Dhahran, Saudi Arabia, for this work.

References

[1]Tauber, M. E., and Menees, G. P., "Aerothermodynamics of Transatmospheric Vehicles," AIAA Paper 86-1257, June 1986.

[2]Krause, J. M., Hartmann, G. L., and Ianculescu, G. D., "Active Thermal Control for Hypersonic Vehicles," *Proceedings of the 29th IEEE Conference on Decision and Control*, Vol. 6, IEEE Control System Society, Honolulu, HI, 1990, pp. 3347, 3348.

[3]Krause, J. M., Hartmann, G. L., and Ianculescu, G. D., "Thermal Control of Hypersonic Vehicle Propulsion," *Proceedings of the American Control Conference*, Vol. 3, Green Valley, AZ, 1991, pp. 2961–2966.

[4]Reich, G., Hinger, J., and Huchler, M., "Thermal Protection

Systems for Hypersonic Transport Vehicles," Twentieth Intersociety Conference on Environmental Systems, Williamsburg, VA, July 1990.

[5]Rainey, S. M., and Veziroglu, T. N., "Computer Modelling and Comparison of Hydrogen-Fueled and Methane-Fueled Hypersonic Vehicles," *International Journal of Hydrogen Energy*, Vol. 17, No. 1, 1992, pp. 53–61.

[6]Vinh, N. X., "Optimal Trajectories in Atmospheric Flight," Elsevier, Amsterdam, 1981.

[7]Al-Garni, A. Z., "Performance and Control of Ascending Trajectories to Minimize Heat Load for Transatmospheric Aero-Space Planes," Ph.D. Dissertation, Dept. of Aerospace Engineering, Univ. of Maryland, College Park, MD, Aug. 1991.

[8]Barlow, J. B., and Al-Garni, A. Z., "Ascending Trajectories Performance and Control to Minimize Heat Load for the Transatmospheric Aero-Space Plane," AIAA Paper 90-2828, Aug. 1990.

[9]Anderson, J. D., Jr., "Hypersonic and High Temperature Gas Dynamics," McGraw–Hill, New York, 1989.

[10]Schilichting, H., "Boundary-Layer Theory," 7th ed., McGraw–Hill, New York, 1979, p. 599.

[11]Roberson, J. A., and Crowe, C. T., "Engineering Fluid Mechanics," 3rd ed., Houghton Miftlin, Boston, MA, 1980, pp. 694, 695.

[12]Van Wylen, G. J., and Sonntag, R. E., "Fundamentals of Classical Thermodynamics," 3rd ed., Wiley, New York, 1985, pp. 103, 651.

[13]Lide, D. R., "CRC Handbook of Chemistry and Physics," 72nd ed., CRC Press, Boca Raton, FL, 1992, pp. 6-111, 6-154–158.

[14]Cox, K. E., and Williamson, K. D., Jr., "Hydrogen: Its Technology and Implications," *Transmission and Storage*, Vol. II, CRC Press, Boca Raton, FL, 1977, p. 52.

Progress in Astronautics and Aeronautics Series

35 field experts present the latest findings

Structural Optimization: Status and Promise

Manohar P. Kamat, editor

1993, 896 pp, illus, Hardback
ISBN 1-56347-056-X
AIAA Members $74.95 Nonmembers $109.95
Order #: V-150(945)

This new book serves as an advanced level text to students and researchers with a basic knowledge of the techniques of optimization. It provides an in-depth assessment of the state-of-the-art in structural sizing and shape optimization including the emerging methods; and the promise that this knowledge holds through its impact on the design of complex spacecraft, aircraft and marine structures.

The initial chapters are devoted to a discussion of the theoretical bases of the optimization techniques for size and shape optimization including topics dealing with constraint approximations, sensitivity analysis of linear and nonlinear structures and the emerging methods of optimization. The latter chapters are devoted to the optimization process in practice including available software and tools for optimization.

Place your order today! Call 1-800/682-AIAA

AIAA
American Institute of Aeronautics and Astronautics
Publications Customer Service, 9 Jay Gould Ct., P.O. Box 753, Waldorf, MD 20604
FAX 301/843-0159 Phone 1-800/682-2422 9 a.m. - 5 p.m. Eastern

Sales Tax: CA residents, 8.25%; DC, 6%. For shipping and handling add $4.75 for 1-4 books (call for rates for higher quantities). Orders under $100.00 must be prepaid. Foreign orders must be prepaid and include a $20.00 postal surcharge. Please allow 4 weeks for delivery. Prices are subject to change without notice. Returns will be accepted within 30 days. Non-U.S. residents are responsible for payment of any taxes required by their government.